Solvent Effects in the Polyethylene Terephthalate Surface Modification by Cold Argon Plasma-Induced Grafting Polymerization of Methacrylic Acid

Laishun Shi, Yanpu Liu, Luyan Wang

School of Chemistry and Chemical Engineering, South Campus, Shandong University, Jinan 250061, People's Republic of China

Received 8 February 2009; accepted 14 December 2009
DOI 10.1002/app.32018
Published online 29 March 2010 in Wiley InterScience (www.interscience.wiley.com).

ABSTRACT: We studied the surface modification of polyethylene terephthalate (PET) by grafting with methacrylic acid (MAA) through plasma-induced polymerization method. The results show that the grafting yield increases with the increase of reaction temperature. The grafting yield is in proportion to the increase of monomer concentration. The grafting yield increases along with the prolonging of reaction time. The solvent has great influence to the grafting reaction. The grafting yield increases with the increase of volume ratio *R*, which is defined by the volume of water to the volume of alcohol, when using alcohol and water as mixed solvent. The grafting yield is not zero when only using methanol, ethanol or isopropanol as the solvent. The red shift in UV spectrum could be ascribed to different reactive activities of MAA in different solvents, which also can explain the change trend of the grafting yield. The UV-vis absorbance difference and the FTIR integrated peak area of the C=O stretching increase steadily with the increase of grafting yield, which are almost linear relationship. It was confirmed that MAA was grafted onto the PET surface in terms of UV-vis spectrophotometric, FTIR and atomic force microscopy analysis. © 2010 Wiley Periodicals, Inc. J Appl Polym Sci 117: 1460–1468, 2010

Key words: plasma polymerization; solvent effects; surface modification; grafting copolymerization

INTRODUCTION

Traditionally, the flame retardancy of a polymer can be achieved by several methods such as by copolymerization or by blending, as well as by treatment with flame retardant finishes.[1–3] Each of these methods has certain inherent disadvantages. For example, the mechanical properties of the polymer materials can be reduced. For transparent materials, transparency can be decreased. Cold plasma is an interesting technology which can be used to modify the surface properties of macromolecule materials to meet certain requirements, e.g., adhesion, printing ability of polymer film, dying ability, hydrophilicity and hydrophobicity. Furthermore, plasma has the advantage of modifying only the surface properties of polymer, without affecting the bulk properties. So far, a number of literatures have reported the polymerization of acrylic acid induced by plasma.[4–9] In previous articles,[10–12] we reported that an attempt had been made to achieve flame retardancy to polymers by grafting with acrylic acid induced by plasma. Based on EVA copolymer with different vinyl acetate (VA) contents (%), it was found that the grafting yield was influenced by the plasma treatment conditions and grafting reaction conditions when EVA copolymer grafted with acrylic monomers. The grafted sample was then neutralized to $-COO^-Na^+$ from $-COOH$ in NaOH aqueous solution. The flame retardancy of the grafted sample was characterized. It was found that the time to ignition of the grafted sample was extended. The Limiting Oxygen Index and char residue were raised. It indicates that the side group of $-COO^-Na^+$ in the grafted layer not only can be charring on the thermal degradation stage, but also can promote the substrate polymer to charring. Therefore, in this article we choose methacrylic acid (MAA) as monomer to graft onto the surface of polyethylene terephthalate (PET) to get the purpose of flame retardancy.

As far as our knowledge goes, only a few literatures have involved the influence of mixed solvent to plasma-induced grafting polymerization.[13–17] Therefore, this article studied the influence of grafting condition on the grafting yield, especially the solvent's influence. To study the inherent essence of mixed solvent to the influence of plasma-induced grafting polymerization, we further investigated the reaction system by UV-vis spectroscopy. The grafted samples were characterized by UV-vis

Correspondence to: L. Shi (LSHUNSH@sdu.edu.cn).

spectrophotometric, FTIR and atomic force microscopy (AFM) analysis.

EXPERIMENTAL

Sample preparation and reagent

PET film was commercial film. The thickness of the specimen is 0.1 mm. Before positioning the four PET films (40 mm length with different width) on the ground electrode of plasma, it was necessary (a) to wash the films with a nonionic detergent solution, (b) to rinse them with deionized water and chloroform, and then (c) to dry them overnight in air. Argon (Jinan DEYANG Gas Factory) supplied in 99.99% purity was used without further purification. MAA and others were of analysis reagent grade and used without further purification.

Low temperature radio frequency plasma treatment

A bell-shaped plasma reactor with a Φ 200 $\times$ 250 mm chamber was made by Changzhou SHITAI Plasma Technology Factory. The glow discharge was generated inner-capacitively, operating at 13.56 MHz. A radio frequency generator of 13.56 MHz was connected to the upper electrode; the lower was grounded. Argon was fed to the chamber through a needle valve. Pump-out was usually at the base of the bell jar. The flow rate was measured with a mass flow meter (Model D07-7/ZM, Jianzhong Machinery Factory, Beijing) and the vacuum in the chamber was controlled by a vacuum pressure gauge (Model ZD0-2). The reaction system was pumped down to 0.8 Pa or lower. Argon, adjusted to a desired flow rate, was introduced into the chamber. Once the pressure remained constant of 25–30 Pa, the glow was initiated at the desired power for certain treated time. The system was at room temperature when argon plasma was applied. After plasma treatment, the vacuum chamber simply vents to the atmosphere.

PET grafting reaction procedure

The specimens were cut into different sizes. Before grafting, a sample was weighed and treated by argon plasma. The reaction conditions of plasma treatment were as follows: time 3 min; power 70W; pressure 28 Pa. The sample was then immersed into the mixed solvent containing MAA at different reaction temperature. The solution was deaerated by nitrogen to remove oxygen before grafting. After grafting, the sample was extracted with a Soxhlet extractor in acetone to remove the homopolymer and monomer.

The grafting yield (G) was calculated according to the equation

$$G(\%) = (M_g - M_0)/M_0$$

where M_0 and M_g represent the mass of specimen before and after grafting, respectively.

Property evaluation

UV-vis spectroscopy analysis

UV-vis spectroscopy measurements were performed in a TU-1800PC UV-vis spectrophotometer (Beijing Puxi Tongyong Instrument Company, Beijing, China). A complete spectrum of the grafted PET samples could be obtained in the range of 200–1000 nm.

FTIR analysis

FTIR spectra were obtained using a Bruker Tensor-27 FTIR spectrophotometer. FTIR spectra were recorded from 400 to 4000 cm^{-1} wavenumber range with averaging 32 scans at a resolution of 4 cm^{-1}.

Surface morphology study

AFM was used to determine surface topography and roughness of the plasma-treated samples. AFM analysis was performed on a NanoScope IIIa MultiMode AFM (Veeco).

RESULTS AND DISCUSSION

Factors affecting the grafting reaction yield

Reaction temperature

The reaction conditions were as follows: time of plasma treatment 3 min; power of plasma treatment 70W; time of grafting 5 h; monomer concentration of MAA in aqueous solution 15%. Figure 1 represents the grafting yield versus reaction temperature (T) for PET grafting with methacrylic acid (abbreviated PET-*g*-MAA). As shown in Figure 1, the grafting yield increases slowly with the increase of reaction temperature when the reaction temperature is below 90°C. The grafting yield increases sharply when the reaction temperature reaches the boiling temperature 103°C of monomer aqueous solution.

Reaction time

The reaction conditions were as follows: time of plasma treatment 3 min; power of plasma treatment 70W; temperature of grafting 103°C; monomer concentration of MAA in aqueous solution 15%. Figure 2 represents the grafting yield versus reaction

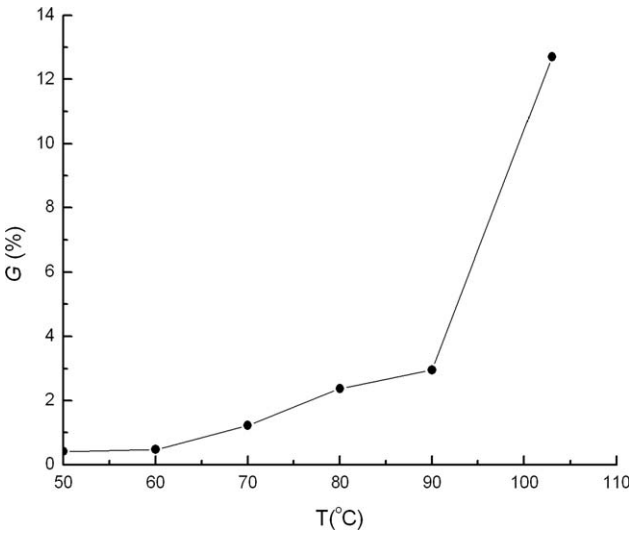

Figure 1 The grafting yield versus reaction temperature for PET-*g*-MAA.

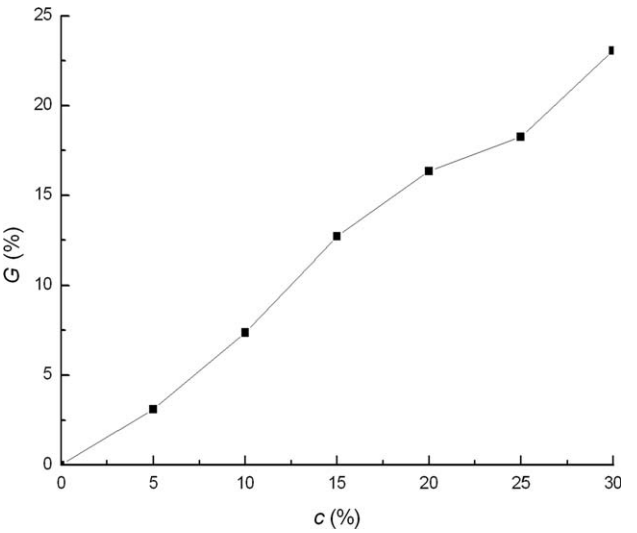

Figure 3 The grafting yield versus monomer concentration for PET-*g*-MAA.

time (*t*) for PET grafting with MAA. As shown in Figure 2, the time of grafting has a notable influence on the grafting yield. The grafting yield increases along with the extension of the reaction time during the grafting polymerization.

Concentration of monomer

The reaction conditions were as follows: time of plasma treatment 3 min; power of plasma treatment 70W; temperature of grafting 103°C; time of grafting 5 h. Figure 3 represents the grafting yield versus concentration of monomer (*c*) for PET grafting with MAA. As shown in Figure 3, the grafting yield increases steadily with the increase of monomer concentration.

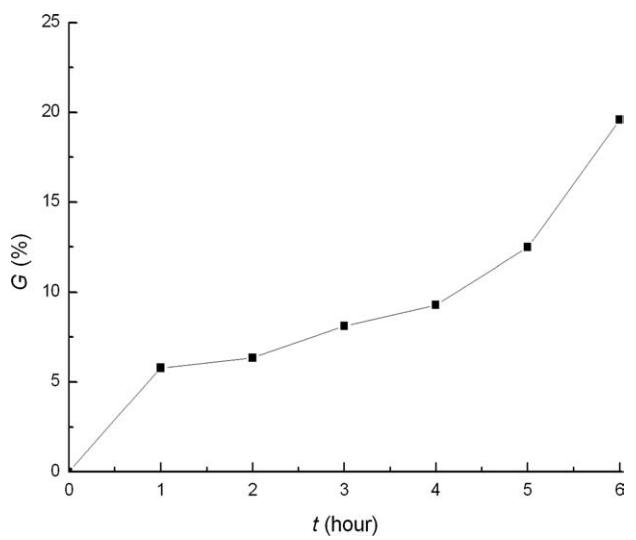

Figure 2 The grafting yield versus reaction time for PET-*g*-MAA.

Solvent

The reaction conditions were as follows: time of plasma treatment 3 min; power of plasma treatment 70W; monomer concentration 15%; boiling temperature of mixed solvent solution; time of grafting 5 h. The boiling temperature solution was mixed by methanol, ethanol or isopropanol with water. The volume ratio (*R*) is defined by the volume of water to the volume of methanol, ethanol or isopropanol.

Figure 4 shows the grafting yield versus *R* for PET grafting with MAA. The grafting yield increases steadily with the increase of *R*. The grafting yields are equal each other when *R* equals two by using methanol, ethanol or isopropanol mixed with water. The three lines are intersected at one point in Figure 4. It is also found that the grafting yield is not zero when *R* is zero. That is to say, the grafting yield is not zero when only using methanol, ethanol or isopropanol as the solvent.

Previous researchers have realized the solvent effect in plasma-induced polymerization, that the monomer polymerizes more rapidly in an aqueous medium and more slowly in organic solvents.[13,14] Osada et al.[13] reported that a significant increase in the electrical conductivity was detected when dimethylformamide was exposed to plasma, and the presence of both ions and radicals was considered. Huang et al.[16] reported that different solvent compositions, that is, water, methanol, benzene, and water/methanol, were used as reaction media, and water showed a much higher polymerization rate than the organic solvents. Based on the hydrophilicity of the active species, a mechanism explaining the solvent effect in plasma-induced graft polymerization was examined.

In this study, we also investigated the solvent effect in a graft polymerization system. It is found that the grafting yield is smaller by using mixed solvent of alcohol and water than by using water as solvent. At the same time, the following change trend of grafting yield can be found at the same volume ratio R by using mixed solvent.

$$(\text{ethanol} + \text{water}) \geq (\text{isopropanol} + \text{water}) \geq (\text{methanol} + \text{water})$$

To further investigate the influence of solvent to the grafting yield, we studied the UV spectra of MAA in different solvents. For MAA, it has n→π* and π→π* transitions in the UV range. Figure 5 gives the UV spectra of MAA in different ethanol solvents (monomer concentration 15%).

Shifts in the position of absorption bands from one solvent to another are mainly caused by differences in the solvation energies of the solute in the ground and excited electronic states.

For π→π* band, it is a rather broad band with a high intensity, occurring in the neighborhood of 220–250 nm. Its position is quite solvent sensitive. Moving an electron from the ground state to an excited state configuration typically leads to an excited state that is more polar than the ground state and more sensitive to solvent effects. For π→π* excited states, dipole-dipole interactions and hydrogen bonding with solvent molecules lead to lower the energy of the excited state more than the ground state with the result that the λ_{max} increases (red shift) about 4 nm from a less interactive solvent like ethanol (235 nm, see curve E) to more interactive solvent like water (239 nm, see curve K). The red shift in UV spectrum could be ascribed to different reactive activities of MAA in different solvents, which also can explain the change trend of the grafting yield in Figure 4.

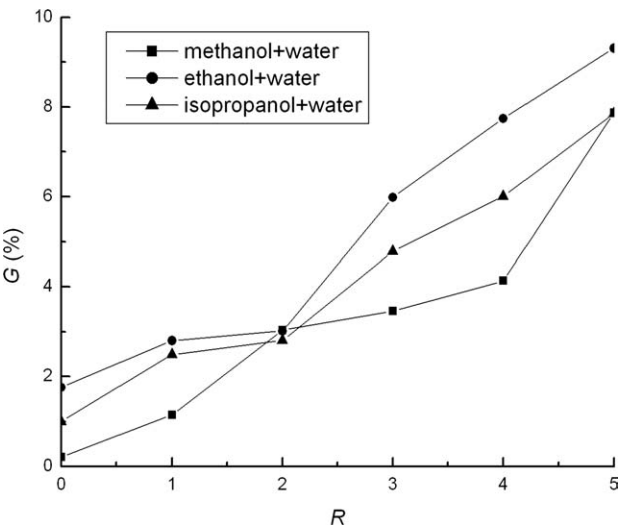

Figure 4 The grafting yield versus volume ratio R for PET-*g*-MAA.

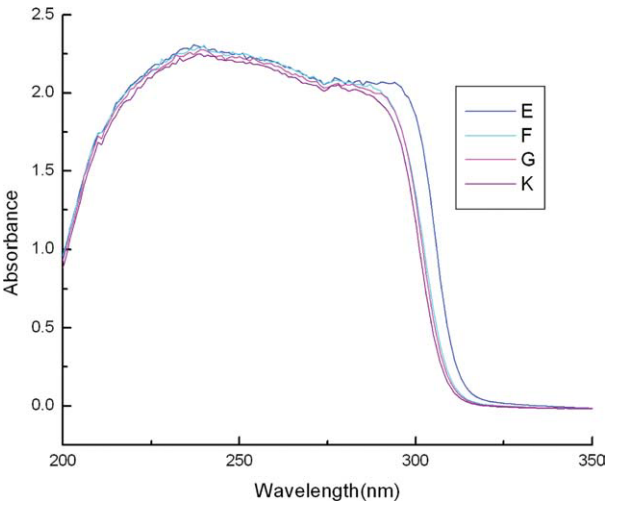

Figure 5 The UV spectra of methacrylic acid in different solvents (E, ethanol $R = 0$; F, ethanol and water $R = 1$; G, ethanol and water $R = 5$; K, water). [Color figure can be viewed in the online issue, which is available at www.interscience.wiley.com.]

For n→π* band, it is a rather broad band with a low intensity, occurring near 270–310 nm. Its position is also quite solvent sensitive. Changing from a less polar solvent to a more polar one could result in a significant hypsochromic shift (blue shift) in the position of the n→π* transition. It has been shown that hydroxylic solvents with comparable dielectric constants cause a large blue shift than nonhydroxylic polar solvents. The larger shifts caused by hydroxylic solvents are attributed in part to greater hydrogen bonding to the carbonyl oxygen lone pairs than to the π* electrons, thus lowering the energy of the ground state relative to that of the excited state.[18,19] By comparing with curve E, the curve F, G, and K produce a blue shift of 7, 9, and 12 nm, respectively.

Figure 6 gives the UV spectra of MAA in different isopropanol solvents (monomer concentration 15%). For π→π* excited states, dipole-dipole interactions and hydrogen bonding with solvent molecules lead to lower the energy of the excited state more than the ground state with the result that the λ_{max} increases (red shift) about 2 nm from a less interactive solvent like isopropanol (237 nm, see curve H) to more interactive solvent like water (239 nm, see curve K). The red shift in UV spectrum could be ascribed to different reactive activities of MAA in different solvents, which also can explain the change trend of the grafting yield in Figure 4. For n→π* band, by comparing with curve H, the curve I, J, and K produce a blue shift of 5, 6, and 10 nm, respectively.

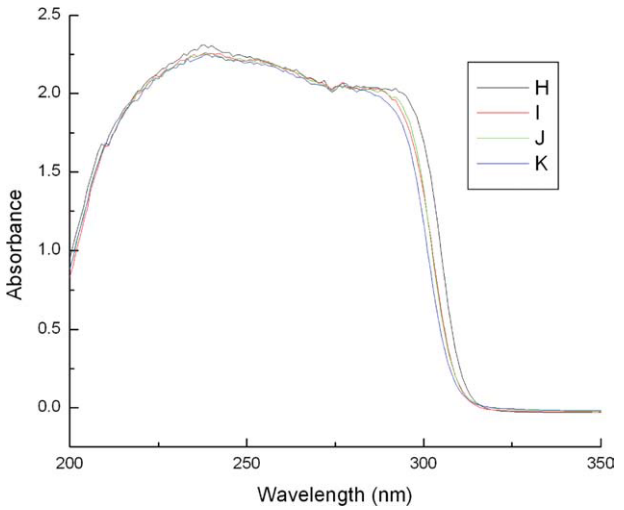

Figure 6 The UV spectra of methacrylic acid in different solvents (H, isopropanol $R = 0$; I, isopropanol and water $R = 1$; J, isopropanol and water $R = 5$; K, water). [Color figure can be viewed in the online issue, which is available at www.interscience.wiley.com.]

Figure 7 gives the UV spectra of MAA in different methanol solvents (monomer concentration 15%). For $\pi \rightarrow \pi^*$ excited states, dipole-dipole interactions and hydrogen bonding with solvent molecules lead to lower the energy of the excited state more than the ground state with the result that the λ_{max} increases (red shift) about 1 nm from a less interactive solvent like methanol (238 nm, see curve B) to more interactive solvent like water (239 nm, see curve K). The red shift in UV spectrum could be ascribed to different reactive activities of MAA in different solvents, which also can explain the change trend of the grafting yield in Figure 4. For $n \rightarrow \pi^*$ band, by comparing with curve B, the curve C, D, and K produce a blue shift of 5, 9, and 13 nm, respectively.

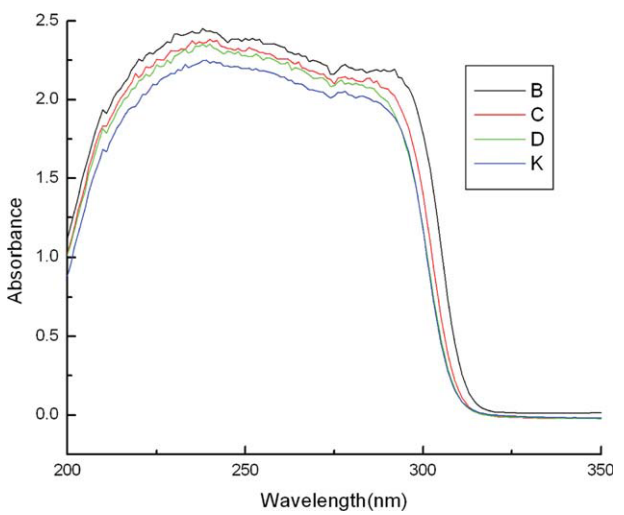

Figure 7 The UV spectra of methacrylic acid in different solvents (B, methanol $R = 0$; C, methanol and water $R = 1$; D, methanol and water $R = 5$; K, water). [Color figure can be viewed in the online issue, which is available at www.interscience.wiley.com.]

If we use the data of 235, 237, and 238 nm found in Figures 5–7 to explain the change trend of grafting yield in different solvents of ethanol, isopropanol and methanol ($R = 0$) in Figure 4, a contradicted result could be led. In fact, the grafting polymerization reaction may be also associated with the stereohindrance effect of solvent, the ability of swelling of PET in different solvents, and the solvent polarity. The factors to influence the grafting yield in different solvents are manifold, and need further investigation.

Characterization of the prepared PET-*g*-MAA

Characterization by UV-vis spectroscopy

Figure 8 illustrates the UV-vis spectra of PET grafted with MAA at different grafting yields. It can be seen that there is no absorption in the visible light range. However, there is a strong absorption in the UV light range. The absorption peaks can be assigned to $n \rightarrow \pi^*$ absorption at 298 nm and the ^{1}Lb aromatic transition at 238 nm. Both bands are bathochromically shifted and considerably increased in intensity due in part to conjugation of the benzene π electrons with the π electrons of the carbonyl group.[18] Figure 9 gives the absorbance difference ($A = A_{298nm} - A_{800nm}$) vs. grafting yield for PET grafted with MAA. As shown in Figure 9, the absorbance increases steadily with the increase of grafting yield, which can prove that MAA has been grafted on the surface of PET.

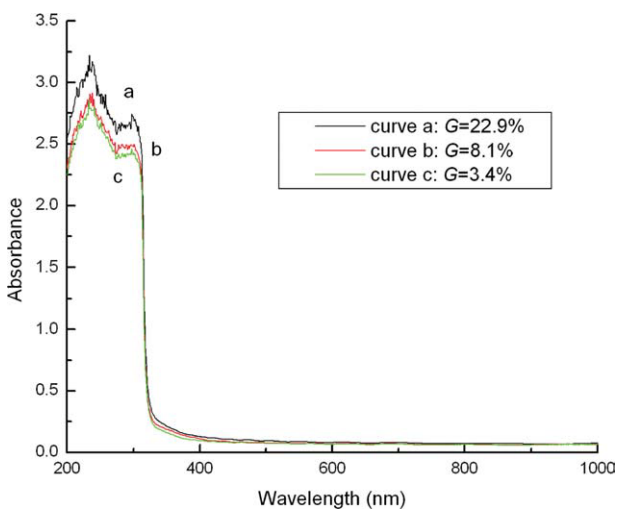

Figure 8 UV-vis spectra of PET-*g*-MAA. [Color figure can be viewed in the online issue, which is available at www.interscience.wiley.com.]

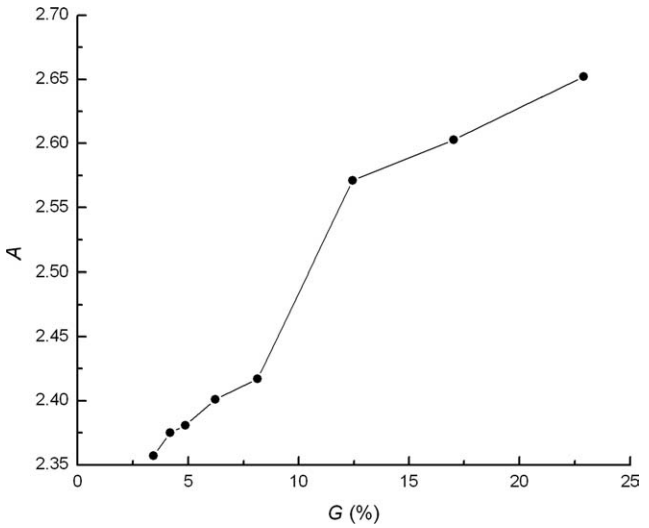

Figure 9 Absorbance difference vs. grafting yield for PET grafted with MAA.

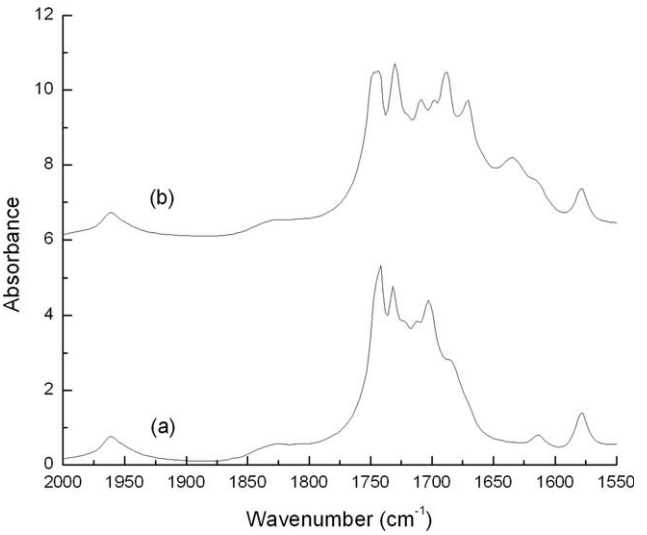

Figure 11 FTIR spectra of PET samples (a) virgin PET; (b) PET-*g*-MAA.

Characterization by FTIR analysis

The FTIR spectra of PET samples are shown in Figure 10. Curve a and b represent untreated PET, and PET grafted with MAA (PET-*g*-MAA, $G = 22.9\%$), respectively. Curve b is shifted up by six absorbance unit for better viewing, since in the absence of a shift the curves overlap. As shown in curve a, the absorption near 3431 cm^{-1} is assigned to the O—H stretching at the end group of PET molecule chain. The absorption near 3102 cm^{-1} is assigned to the aromatic C—H stretching. The absorption near 2970 cm^{-1} is assigned to the methylene nonsymmetry stretching. The absorption near 2815 cm^{-1} is assigned to the methylene symmetry stretching. The strong absorption band near 1775–1625 cm^{-1} is assigned to the C=O stretching in esters and carboxylic acids. The absorptions near 1614 and 1578 cm^{-1} are assigned to the benzene ring stretching in aromatic compounds (sharp peak). The absorptions near 1524, 1505, 1471, and 1454 cm^{-1} are assigned to the aromatic C=C stretches (four bands) in phenyl. The absorptions near 1412 and 1388 cm^{-1} are assigned to the OH in-plane bending in carboxylic acids. The absorptions near 1243, 1146, 1135, 1110, and 1083 cm^{-1} are assigned to the CH in-plane bending (five bands) in phenyl. The absorption near 972 cm^{-1} is assigned to the C—OH deformation in carboxylic acids. The strong absorption near 732 cm^{-1} is assigned to the CH out-of-plane bending

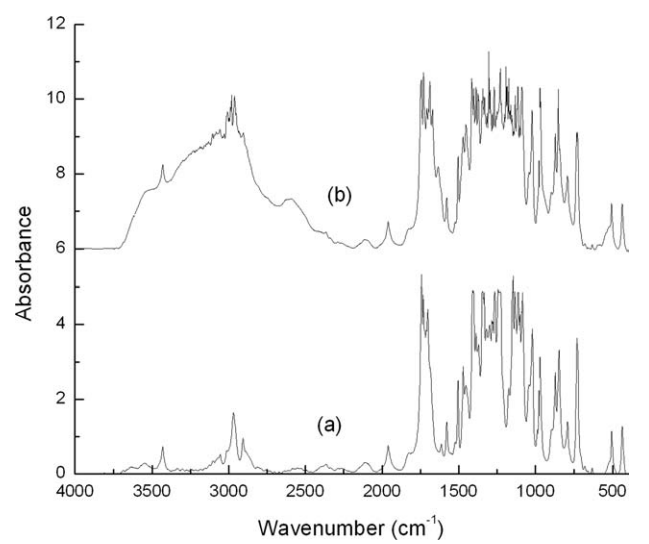

Figure 10 FTIR spectra of PET samples (a) virgin PET; (b) PET-*g*-MAA.

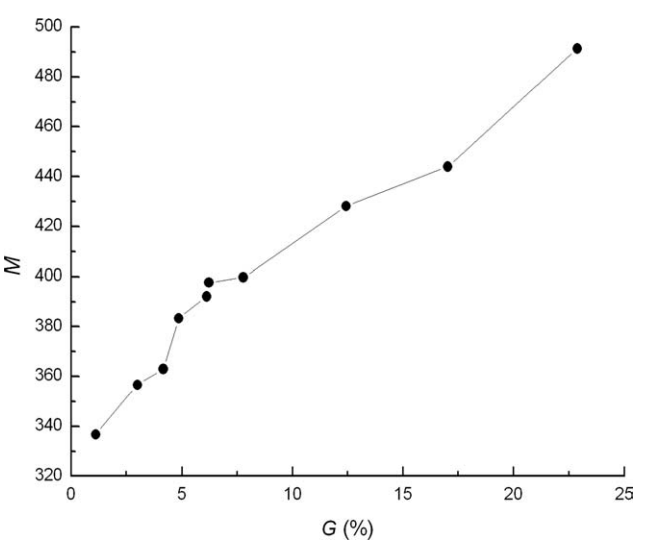

Figure 12 Integrated peak area vs. grafting yield for PET grafted with MAA.

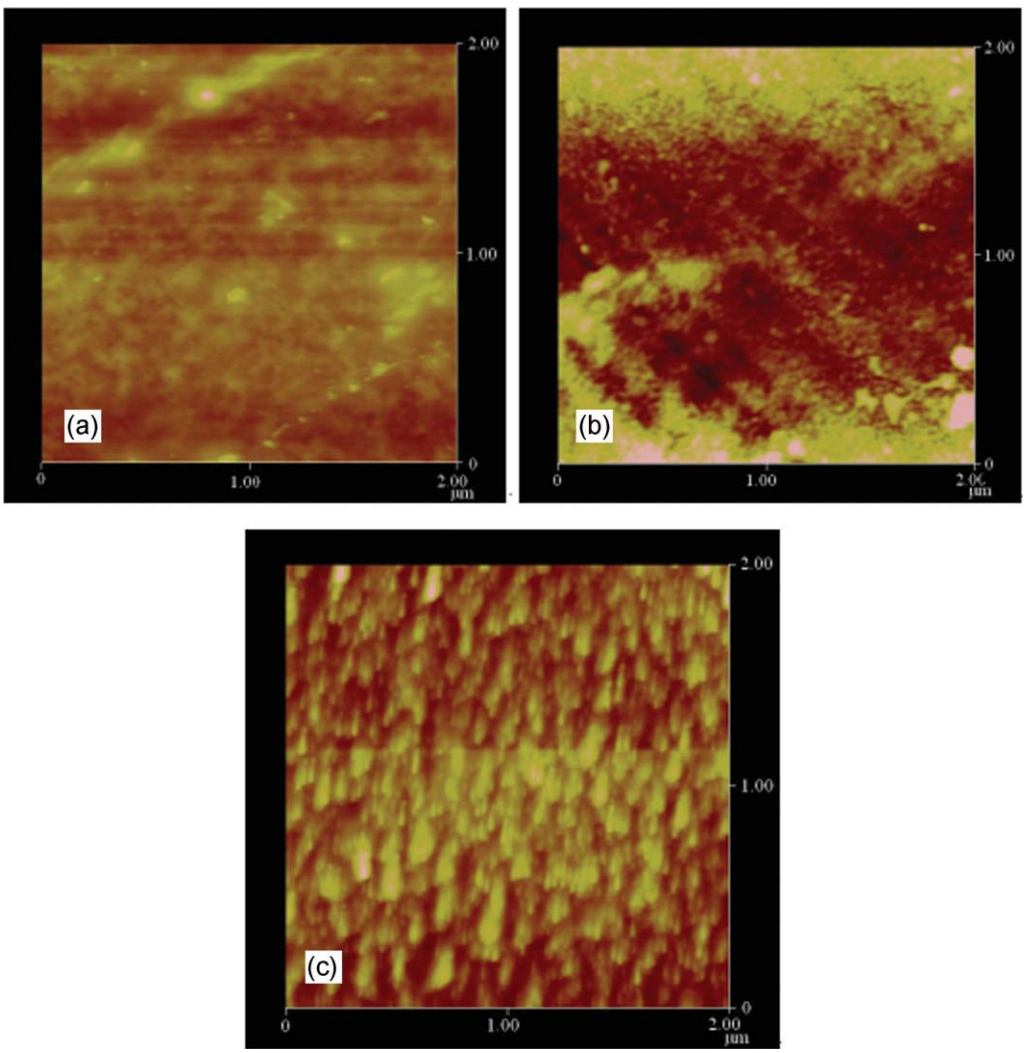

Figure 13 The AFM 2D micrographs of PET samples: (a) virgin PET; (b) PET treated by argon plasma; (c) PET-*g*-MAA. [Color figure can be viewed in the online issue, which is available at www.interscience.wiley.com.]

in phenyl. The absorption near 506 cm^{-1} is assigned to the O—C=O bend in esters and carboxylic acids. The absorption near 437 cm^{-1} is assigned to the ring deformation in phenyl.

For PET-*g*-MAA sample (see curve b), all absorption peaks of PET still exist. However, there are three apparent differences. Firstly, the broad band at 3200–3700 cm^{-1} is the characteristic of carboxylic acids. Secondly, the absorption near 2989 cm^{-1} is assigned to the CH stretch in C—CH_3 compounds of MAA. Thirdly, the difference of strong absorption band at 1775–1625 cm^{-1} between curve a and curve b.

Figure 11 illustrates the local amplificatory FTIR spectra at 1775–1625 cm^{-1}. Curve a and b represent virgin PET, and PET grafted with MAA (PET-*g*-MAA, $G = 22.9\%$), respectively. Curve b is shifted up by six absorbance unit for better viewing, since in the absence of a shift the curves overlap. For curve a, the absorptions near 1742, 1732, and 1712 cm^{-1} are assigned to the C=O stretching in esters. The absorption near 1703 cm^{-1} is assigned to the C=O stretching in carboxylic acids. For curve b, the absorptions near 1744, 1730, and 1709 cm^{-1} are assigned to the C=O stretching in esters. The absorptions near 1698, 1688, and 1671 cm^{-1} are assigned to the C=O stretching in carboxylic acids. By comparing curve a and b, the absorption intensity near 1698, 1688, and 1671 cm^{-1} is enhanced, and the wavenumber shifted to lower side. All those indicate that MAA is grafted onto the surface of PET.

The strong absorption bands of the C=O stretch in esters and carboxylic acids can be integrated in the range of 1545–1878 cm^{-1} by using FTIR software. Figure 12 represents the integrated peak area (M) as a function of the grafting yield for PET-*g*-MAA samples. As shown in Figure 12, the integrated peak

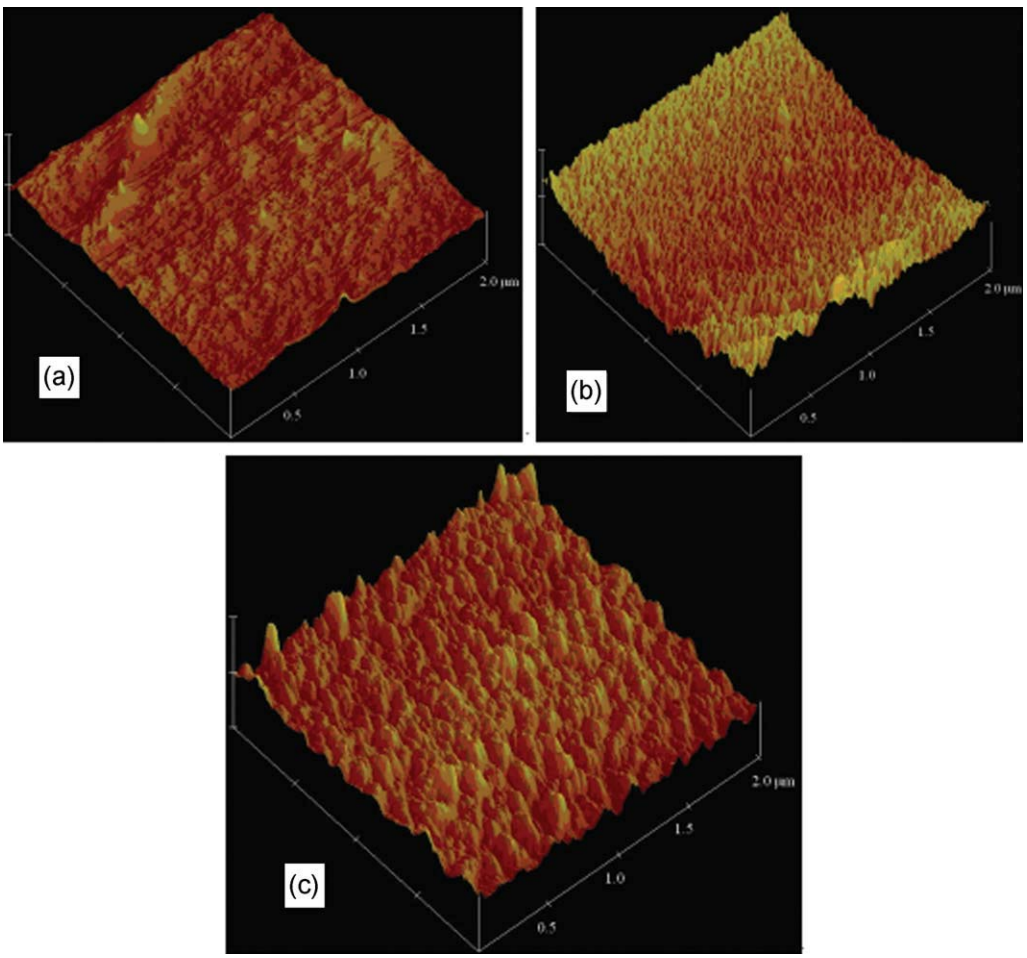

Figure 14 The AFM 3D topographic representations of PET samples: (a) virgin PET; (b) PET treated by argon plasma; (c) PET-*g*-MAA. [Color figure can be viewed in the online issue, which is available at www.interscience.wiley.com.]

area increases steadily with the increase of grafting yield, and almost displays linear relationship. This also can prove that MAA has been grafted onto the surface of PET.

Characterization by surface morphology

AFM 2D micrographs and AFM 3D micrographs for different PET samples are shown in Figures 13 and 14, respectively. In the figures, picture (a) is virgin PET. Picture (b) is argon plasma treated PET under the condition of pressure 28Pa, power 70W, and treated time 3 min. Picture (c) is PET-*g*-MAA sample under the grafting condition of MAA concentration 15%, reaction temperature 103°C, and reaction time 5 h.

Untreated PET surface is characterized by smooth and low surface roughness [Figs. 13(a) and 14(a)]. Argon plasma treatment causes a change in surface roughness as it promotes etching processes [Figs. 13(b) and 14(b)]. A great number of small peaks are generated, thus increasing surface roughness. For PET-*g*-MAA sample, the surface morphology is obviously different from that of virgin PET, and indicates the formation of new structures [Figs. 13(c) and 14(c)]. It indicates that MAA is grafted onto the PET surface.

CONCLUSIONS

1. Successful graft copolymerization of MAA on the surface of PET films, which previously treated by argon plasma, was confirmed through the analysis of UV-vis spectrophotometric, FTIR and AFM analysis.
2. The solvent has great influence to the grafting reaction. The grafting yield increases with the increase of volume ratio *R* when using alcohol and water as mixed solvent. The grafting yield is not zero when only using methanol, ethanol or isopropanol as the solvent. A mechanism explaining the solvent effect is proposed.

3. The grafting yield has the following trend for PET grafting with MAA at the same volume ratio by using mixed solvent.

$$(\text{ethanol} + \text{water}) \geq (\text{isopropanol} + \text{water}) \geq (\text{methanol} + \text{water})$$

4. The UV-vis absorbance difference ($A = A_{298\text{nm}} - A_{800\text{nm}}$) increases steadily with the increase of grafting yield. The FTIR integrated peak area of the C=O stretching also increases steadily with the increase of grafting yield. There is almost linear relationship.

References

1. Gui, H.; Zhang, X. H.; Liu, Y. Q.; Dong, W. F.; Wang, Q. G.; Gao, J. M.; Song, Z. H.; Lai, J. M.; Qiao, J. L. Compos Sci Technol 2007, 67, 974.
2. Chattopadhyay, D. K.; Webster, D. C. Prog Polym Sci 2009, 34, 1068.
3. Yildiz, B.; Seydibeyoglu, M. O.; Guner, F. S. Polym Degrad Stabil 2009, 94, 1072.
4. Konig, U.; Nitschke, M.; Menning, A.; Eberth, G.; Pilz, M.; Arnhold, C.; Simon, F.; Adam, G.; Werner, C. Colloid Surf B: Biointerfaces 2002, 24, 63.
5. Zhang, J.; Feng, X. F.; Xie, H. K.; Shi, Y. C.; Pu, T. S.; Guo, Y. Thin Solid Films 2003, 435, 108.
6. Vilani, C.; Weibel, D. E.; Zamora, R. R. M.; Habert, A. C.; Achete, C. A. Appl Surf Sci 2007, 254, 131.
7. Yaman, N.; Ozdogan, E.; Seventekin, N.; Ayhan, H. Appl Surf Sci 2009, 255, 6764.
8. Pandiyaraj, K. N.; Selvarajan, V.; Rhee, Y. H.; Kim, H. W.; Shah, S. I. Mater Sci Eng C 2009, 29, 796.
9. Wang, C.; Chen, J. R. Appl Surf Sci 2007, 253, 4599.
10. Shi, L. S. Des Monomers Polym 1999, 2, 359.
11. Shi, L. S. Eur Polym J 2000, 36, 2611.
12. Shi, L. S. React Funct Polym 2000, 45, 85.
13. Osada, Y.; Takase, M.; Iriyama, Y. Polym J 1983, 15, 81.
14. Osada, Y.; Takase, M. J Polym Sci Polym Lett Ed 1983, 21, 643.
15. Kuzuya, M.; Kawaguchi, T.; Yanagihara, Y.; Nakai, S.; Okuda, T. J Polym Sci Polym Chem 1986, 24, 707.
16. Huang, J.; Wang, X. L.; Chen, X. Z.; Yu, X. H. J Appl Polym Sci 2003, 89, 3180.
17. Wang, X. L.; Huang, J.; Chen, X. Z.; Yu, X. H. Desalination 2002, 146, 337.
18. Lambert, J. B.; Shurvell, H. F.; Lightner, D. A.; Cooks, R. G. Introduction to organic spectroscopy; Macmillan Publishing Company: New York, 1987; p 270.
19. Hammud, H. H.; Bouhadir, K. H.; Masoud, M. S.; Ghannoum, A. M.; Assi, S. A. J Solution Chem 2008, 37, 895.